# AN INFRARED SURVEY OF GALACTIC SUPERNOVA REMNANTS

Richard G. Arendt
University of Illinois
349 Astronomy Bldg.
1011 W. Springfield
Urbana, IL 61801

Abstract: Presented here are preliminary results from a survey of supernova remnants (SNRs) in the data base collected by the Infrared Astronomical Satellite (IRAS). About one-third of the known galactic SNRs are visible in the IRAS data. Confusion with other sources in the galactic plane prohibits the detection of many remnants. The objects that are detected have similar spectral characteristics and temperatures, except that the three youngest remnants known, Tycho, Kepler, and Cassiopeia A, are distinctly warmer.

## 1. INTRODUCTION

Galactic supernova remnants are usually identified by non-thermal radio spectra, relatively strong polarization, and shell-like morphology. Many SNRs are also observed as x-ray sources. Remnants which are nearby or along paths of low extinction, can often be detected optically as well. However, until the recent work of IRAS, observations of SNRs in the far-infrared ($\lambda \geq 10\mu$) were extremely scarce. This omission in spectral coverage is significant. Most of the IR emission arises from collisionally heated dust. This energy loss may be a major fraction of the total luminosity and can have a significant effect on the evolution of many SNRs (e.g. see Dwek 1981). The presence of this dust is not directly observed in any other wavelength regime.

This paper presents preliminary results of a project to measure flux densities in the infrared for all known galactic SNRs. The full catalog is not yet complete, but the sample is large enough that several trends are apparent. Section 2 describes the process by which the flux densities are measured. Section 3 describes some of the general properties of SNRs in the infrared.

## 2. PROCEDURE

The IRAS satellite provides survey observations in four broad bands centered on 12, 25, 60 and 100$\mu$. These data, in three different formats are being used for this project. The standard Sky Brightness Images (calibrated surface brightness maps with 2′ pixels, see IRAS Explanatory Supplement 1985 for a complete description) are being used for most objects. For 37 SNRs, two-dimensional coadded fields of higher resolution (0ʹ.25 - 1ʹ.0 pixels) are also being used. These coadded fields use the data from all of the satellite's passes over the

https://doi.org/10.1017/S0252921100102684 Published online by Cambridge University Press

selected regions. These maps are processed to yield a flat background over the field. For most of the smallest SNRs (≤ 8′ diameter), we also have one-dimensional co-added data. These data provide the highest resolution, and are suitable for objects which have a high degree of symmetry, or which are not well resolved by the IRAS satellite. These data are in the from of averaged slices across the source in each of the four IRAS bands.

Total flux densities are measured from the images by integrating over the area occupied by the remnant, and subtracting a background level determined by integration over a roughly equal area surrounding the remnant. These integrations are done over both circular and rectangular regions. Obvious bright and unrelated sources are excluded from the process. In cases where only an upper limit can be established, the background is chosen to be the lowest level in the region occupied by the SNR. In most cases there is good agreement between the results from the various data formats and the different integration techniques. The differences in the resulting flux densities are comparable to the variations which arise from alterations of the region over which the background is determined.

## 3. RESULTS

So far we have examined the regions of 70 supernova remnants. Currently the sample is slightly biased towards the brighter and more well known SNRs, and more noticeably towards objects near the galactic center. In 16 regions there is infrared emission clearly associated with the remnant; 30 regions show no infrared emission attributable to the SNRs; and in 24 regions there is emission which may be from the SNR, but the association is uncertain. Confusion with the complex background provided by the galactic plane appears to be a significant problem. The mean distance from the galactic plane for detectable SNRs is 2°.0, while the mean distance for undetected SNRs is 0°.8. However, there are several examples of SNRs at high galactic latitudes in apparently unconfused regions which show no IR emission.

In the most convincing detections the IR emission correlates fairly well with the optical and/or radio emission (e.g. Cygnus Loop, OA 184, RCW 86), or the IR emission correlates with that of shock excited molecules (e.g. IC 443). In several of the uncertain cases, the IR emission is from a relatively small clump which has a suggestive position in relation to the radio morphology (e.g. G 7.7-3.7, Kes 67, G 323.5+0.1).

In most cases where infrared emission is detected from a SNR, the IR luminosity is greater than both the x-ray luminosity and the radio luminosity. This is based on the objects in the present sample for which x-ray fluxes or luminosities are found in the literature. Examination of ~20 such SNRs indicates that only the Crab nebula clearly has its greatest luminosity in a wavelength regime other than the infrared. In SNRs for which only upper limits are obtained, the IR luminosity is not required to be less than the luminosity in other regimes.

The limited spectral information provided by the four IRAS bands is not of great assistance in discriminating SNRs from other infrared

https://doi.org/10.1017/S0252921100102684 Published online by Cambridge University Press

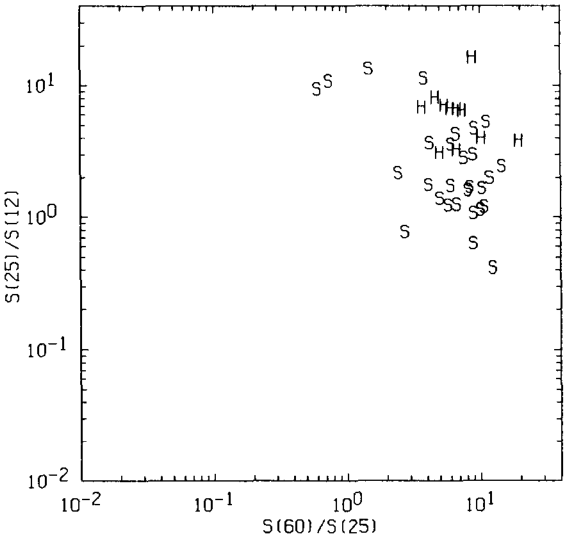


Figure 1

In this color-color diagram S designates an SNR, H designates a compact HII region. There is some tendency for SNRs to appear lower than compact HII regions on this diagram. This reflects somewhat greater $12\mu$ emission (relative) in SNRs than in compact HII regions.

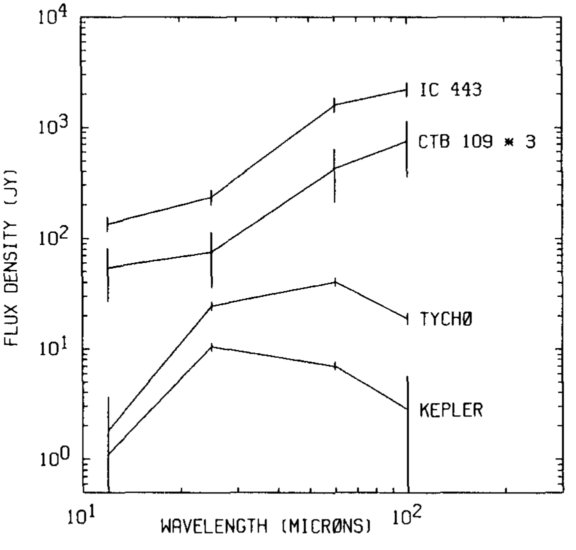


Figure 2

This figure illustrates the difference between the spectra of typical old and young supernova remnants. The spectra of IC 443 and CTB 109 are representative of the spectra of older SNRs. Tycho, and Kepler are typical of young SNRs.

https://doi.org/10.1017/S0252921100102684 Published online by Cambridge University Press

sources. Most SNRs are brightest in the 100$\mu$ band, although it is usually easiest to detect them in the 60$\mu$ band. The same is true for compact HII regions (Chini, et al. 1986, Antonopoulou and Pottasch 1987), which have relative flux ratios that are very similar to those of SNRs. On a color-color diagram involving the longer wavelengths, there is no distinction between SNRs and compact HII regions. A color-color diagram using the shorter wavelengths does show some separation between the two classes of objects, but the separation is not clear enough to use as a discriminator between SNRs and compact HII regions (see figure 1). The separation is due to the tendency of SNRs to have slightly more 12$\mu$ emission (relatively) than compact HII regions. If this effect is real, one cause could be differing amounts of fine structure line emission at 12$\mu$ between the two types of objects. Another possible cause would be an enhancement of very small grains in most SNRs with respect to the distribution of grains found in compact HII regions. Such an enhancement could be the result of sputtering grains down to smaller sizes behind the shock fronts of the SNRs.

The youngest SNRs (Tycho, Kepler, Cas A) show energy distributions which are distinctly different from the older ones (see figure 2). These three all have peak flux densities between 25$\mu$ and 60$\mu$. The dust temperatures derived are about 100K (~40K warmer than most other SNRs). Objects such as these are similar in infrared appearance to planetary nebulae (Pottasch, et al. 1984).

Thanks are extended to Dr. John R. Dickel for his valuable comments and suggestions on the preparation of this paper.

References:

Antonopoulou, E., and Pottasch, S. R., 1987, Astr. Ap., **173**, 108.

Chini, R., Kreysa, E., Mezger, P. G., and Gemünd, H.-P., 1986, Astr. Ap., **154**, L8.

Dwek, E., 1981, Ap. J., **247**, 614.

IRAS Catalogs and Atlases, Explanatory Supplement 1985, edited by Beichman, C. A., Neugebauer, G., Habing, H. J., Clegg, P. E., and Chester, T. J., (Washington D.C.: U. S. Government Printing Office.)

Pottasch, S. R., Baud, B., Beintema, D., Emerson, J., Habing, H. J., Harris, S., Houck, J., Jennings, R., and Marsden, P., 1984, Astr. Ap., **138**, 10.

https://doi.org/10.1017/S0252921100102684 Published online by Cambridge University Press